Geological Society of Malaysia Bulletin 51
June 2005 p.103-121

Petrology and geochemistry of the Sempah volcanic complex : Peninsular Malaysia

Azman A Ghani & Navpreet Singh[1]

Department of Geology
University of Malaya
Kuala Lumpur 50603
Malaysia

[1]Sarawak Shell Berhad,
Locked Bag No.198009, Miri, Sarawak, Malaysia

Abstract: The Sempah volcanic complex is characterized by a sequence of tuffs, rhyolite lava and an orthopyroxene bearing subvolcanic unit exposed along the Selangor-Pahang state boundary. Previous radiogenic dating of the complex using Rb-Sr method yield ages in the range of 211 to 219 Ma and suggests that it may be temporally related to the Triassic Main Range Granites. The two main rock types of the complex are rhyolite and orthopyroxene-bearing rhyodacite. They are porphyritic and have similar phenocryst assemblage (quartz, biotite, K-feldspar and plagioclase) except for the presence of hypersthene in the orthopyroxene-bearing rhyodacite. Geochemically both units are peraluminous, high-K calc alkaline and display S type affinities. Both rhyolite and orthopyroxene rhyodacite are inferred to be individual batches of melt. Although they have very similar SiO_2 content, the two groups display contrasting trends for many of the trace and major element diagrams. High $^{87}Sr/^{86}$ Sr isotope values, different mineral extract proportion in the major elements modelling and non-horizontal trend on the $^{87}Sr/^{86}Sr$ vs.1/Sr plot preclude crystal fractionation as the main process operating in the complex. Modelling confirms that the cause of the chemical diversity between both rocks can be explained by combined assimilation – fractional crystallization (AFC) and that approximately 20% of both magmas were contaminated during emplacement. It is inferred that the water content of the orthopyroxene rhyodacite magma was between 2.5 to 3 % with pressure regime of 3 – 4 kbar and a temperature approximately 800 - 900°C when rapid quenching of the groundmass occurred. The rhyolite magma, however was generated at shallower crustal levels, probably between 700 - 800°C.

INTRODUCTION

The contemporaneous association volcanic or subvolcanic rocks with granitic bodies is not uncommon (Atherton et al., 1979; Norman et al., 1992). The relationship between both volcanic and their granitic counterparts is crucial as the former can indicate the character of near liquidus phases. In addition, the texture and the composition of the phenocrysts can be used to establish the early crystallization history of magma and the composition of the liquid (Atherton et al., 1992). In the Western Belt granite of the Peninsular Malaysia the best known volcanic complex is the Genting Sempah Volcanic Complex, that is related, both temporally and spatially, to the granite. The complex comprises units of tuff, lavas and a distinctive porphyry subvolcanic unit that contains orthopyroxene phenocrysts (Liew 1983; Chakraborty, 1995). The main problem concerning this complex is its peculiar relationship with the adjacent Bukit Tinggi Pluton and the Western Belt Granite as a whole. Liew (1983) bracketed the age of the complex between 219-211 Ma (based on U-Pb zircon data) which imply that it is temporally related to the Western Belt Granite. The objective of this study is to conduct a thorough petrographic and geochemical examination of the rocks of the complex in order to determine the genetic relationship between the rocks and to explain the cause of the chemical variation within the rocks of the complex.

These rocks were referred to as rhyolite (rhyolite in this paper) and as porphyritic pyroxene microgranodiorite (Orthopyroxene Rhyodacite in this paper) respectively by previous workers (Liew, 1983; Haile, 1970). The rocks have been well studied and documented by many workers (Scrivenor, 1931; Alexander, 1968; Shu, 1968). Many of the discussions of the workers centered on the relation of this complex to the Main Range Granite. Hutchison (1973) suggested that the Sempah Complex rocks are not related to the Main Range Granite because of their distinctive different mineralogical and textural nature. He suggested that the Complex is more likely to be related to the roof pendant of greenschist facies metasediments (Selut schist) of Lower Paleozoic age. Liew (1977) stated in his thesis, 'The undeniably pyroclastic nature of the rhyolitic rocks (rhyodacite in this paper) seems to make it clear that they are unlikely to represent a marginal modification of the Main Range granite. Bignell (1972) dated (Rb/Sr whole rock method) the rhyodacite as Carboniferous-Permian and the orthopyroxene rhyodacite as late Silurian – late Devonian. Liew (1977) noted that if this age is accepted, it would reflect a Devonian intrusive episode distinct from the dominant Permian to Triassic intrusions of the Main Range granites. In this paper we report ongoing work on the petrochemistry of the complex. New outcrops from the development of the Karak Highway have enabled us to

study in detail the nature of the contact between these two rocks.

GEOLOGICAL SETTING

The Peninsular Malaysian granites are distributed into three parallel belts, i.e. Western, Central and Eastern belts. They have been grouped into two granite provinces; a Western province consisting of granites confined to the Western Belt with an age range from 200 to 230 Ma (Cobbing et al., 1992) and the Eastern province consisting of granites from both the Eastern and Central belt and aged from 200 to 264 Ma (Cobbing et al., 1992). The Western belt granites are characterised by a huge mountain range extending from Malacca in the south to Thailand in the north which covers the area exceeding 15000 km^2 (**Fig 1**) Two main batholith masses can be distinguished in the Western Belt Granite (Fig.1). These are the Main Range batholith on the eastern flank and the adjacent Bintang batholith immediately to the west. Small intrusive centres are found further to the west. These are called Bukit Mertajam-Kulim, Penang, and Langkawi complexes. Each granitic batholith consists of individual plutons (e.g. Liew, 1983). The Western Belt granite occurs to the west of a belt containing ophiolite- melange association which known as Bentong–Raub line by Hutchison (1975; 1977). Mitchell (1977) interpreted this ophiolite line to mark a Triassic collision suture separating an eastern Malay Peninsula crustal block and western Malay Peninsula crustal block. He proposed that, in such a tectonic reconstruction, the Western Belt granites were formed in a continent collision setting broadly analogous to that of the Tertiary Himalayan leucogranites.

In term of rock types and mineral associations the whole Western belt granite can be divided into three distinct groups. The first group covers about 90% of the total Western Belt granite volume. The main rock type is a coarse to very coarse grained megacrystic biotite muscovite granite. Two phase variants, however, developed almost everywhere and may be volumetrically important (Pitfield et al., 1990; Cobbing et al., 1992; Mursyidah and Azman, 1999). Aplopegmatite and mesogranites are commonly associated with the individual granitic body.

The second group corresponds to the amphibole bearing granite found in several granitic bodies at the northern part of the Western belt granite. The Bintang granite complexes are the best example. Common mineralogical assemblages of this complex are low Al biotite + sphene ± actinolitic hornblende (Liew, 1983; Borhan Doya, 1995). Khoo and Lee (1994) have reported

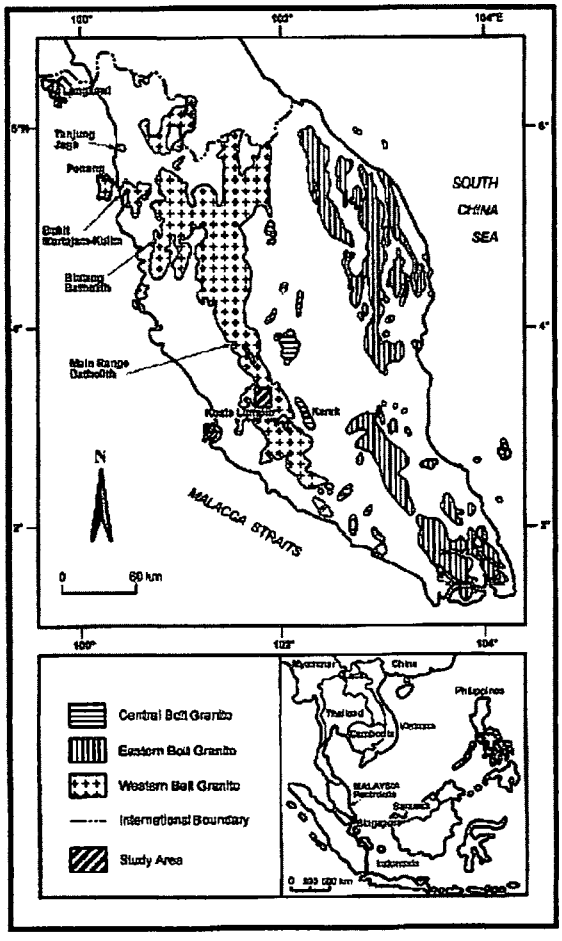

Figure 1: Map of the Peninsular Malaysia show the Western Belt Granites in relation to other granites batholith. Square inset map shows the location of Peninsular Malaysia.

a suite of plutonic rocks consisting of hornblende-biotite quartz monzonite, tonalite, granodiorite and adamellite from northeasternmost Western Belt Granite. Amphibole bearing enclaves have also been reported in the Bujang Melaka Granite (Singh and Yong, 1982).

The third group is the felsic volcanic rocks associated with the Western Belt Granites. The type area is the Genting Sempah Volcanic Complex that is related, both temporally and spatially, to the granite (Cobbing et al. 1992). The Sempah Volcanic Complex occupies the central part of the Western Belt Batholith to the east of Kuala Lumpur city. The Complex intruded the Pre Devonian Selut Schist , Late Devonian to Early Carboniferous Gombak Chert and Permian Sempah Conglomerate which were collectively known as the Bentong Group (Alexander, 1968). The complex comprises units of tuff, lavas and a distinctive porphyritic subvolcanic unit that contains orthopyroxene phenocrysts (Liew, 1983; Chakraborty, 1995). The two main rock types of the Complex are rhyodacite and orthopyroxene bearing rhyodacite (Chakraborty, 1995; Singh and Azman, 2000).

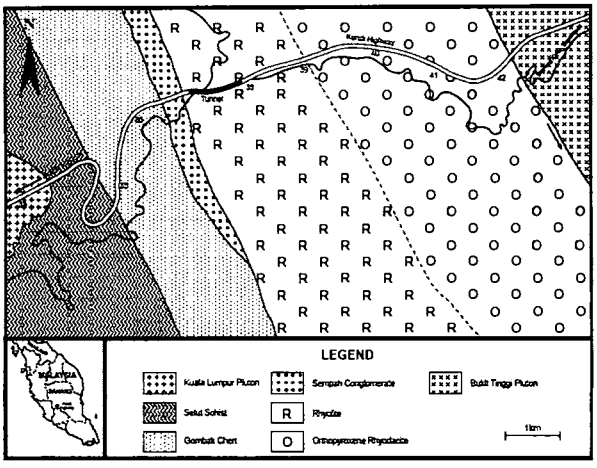

Figure 1: Regional geology map of the Genting Sempah area, showing the relationship between the volcanic Complex (Rhyolite and Orthopyroxene Rhyodacite) and the adjacent Paleozoic metamorphic rocks and the late Triassic granitic rocks. Dashed line represent inferred fault zones, while heavy lines are lithological contact. Lithological contacts for the Selut Schist, Sempah Conglomerate and the Bukit Tinggi pluton are also fault zones

GENERAL GEOLOGY

The Sempah Volcanic Complex is situated on the Selangor-Pahang state boundary primarily along the Kuala Lumpur-Karak Highway **(Fig. 2)**, approximately 38 km from Kuala Lumpur. The complex comprises of two main distinctive porphry subvolcanic unit, that is rhyolite and orthopyroxene rhyodacite, and minor units of tuff, lavas (Liew, 1983; Chakraborthy, 1995). The Complex intruded a group of Lower paleozoic country rocks. Alexander (1968) believed that the whole sequence of country rocks mentioned above (volcanic complex and their country rocks) is a roof-pendant that had resulted from different episodes of granitic intrusions. The western portion of the roof-pendant consists of the Selut Schist. It is overlain by the Gombak Chert along a major fault; which is represented by a zone of sheared rocks (Lee, 1976). A spectacular angular unconformity separates the chert from the overlying Sempah Conglomerate (Lee, 1976). Along a stream on the Genting Highlands slip road, two small bodies of metaconglomerate (Sempah Conglomerate) overlie the volcanic rocks (Chow et al., 1995) implying a post-rhyolite age. A zone of sheared granite separates the volcanics from the Bukit Tinggi Pluton, some 4 km from the eastern portal of the Karak Highway Tunnel.

The rhyolite is present in the western portion of the complex, mainly from km 37 to km 38.2 along the Karak Highway. The best outcrops are located on a new road from the Genting Sempah rest area to Genting Highlands, which is adjacent to the highway. The rock can be recognized in the field based primarily on the occurrence of feldspar phenocrysts. From km 38.2 to km 38.3, there appears to be some change in the rhyolite in which the phenocryst content increases and starts to resemble the orthopyroxene dacite. The supposed contact as proposed by Liew (1977) is the first stream to the west of Sungai Kenyoi, some 200m from the eastern portal of the tunnel. Evident of mixing between both magmas can be found on the road adjacent to the highway, as the rhyolite and orthopyroxene rhyodacite seem to interdigitate.

The complex is also characterized by the presence of quartz and calcite veins and aplite dykes. The latter consists two types of aplite dykes: one that is whitish in appearance while the other is dark grey. Contacts between dykes are sharp and the inclusions of a large orthopyroxene dacite fragment in an aplite dyke indicate that the aplite dykes are later intrusive events. Dark enclaves ranging from 2-10 cm are abundant throughout the complex. Most of the enclaves are rounded except for the presence of stretched enclaves close to the vicinity of shear zones. The stretching feature could have also been caused by magmatic movement. An interesting feature observed is that most enclaves in the orthopyroxene rhyodacite seem to dip (based on the longest axis) towards the southeast. The reason for this is unclear, but there is a possibility that this could be a form of magmatic flow. According to Bacon (1986), the ellipsoidal form displayed

by most enclaves is also evidence for incorporation in a molten state. Liew (1977) mentioned the occurrence of several types of enclaves such as spinel-corundum-sericite-biotite-plagioclase-cordierite, surmicaceous, quartz epidote hornfelsic and hyperstene-quartz-plagioclase-biotite enclaves.

Rare monomineralic clusters of quartz (2 mm) are also present, with each microphenocryst averaging 0.3–0.5 mm in diameter. Inclusions of biotite observed in quartz suggest that quartz was a late crystallizing phase. Many of the phenocrysts are deeply and intricately embayed, usually being filled with groundmass.

Plagioclase occurs as individual euhedral–subhedral

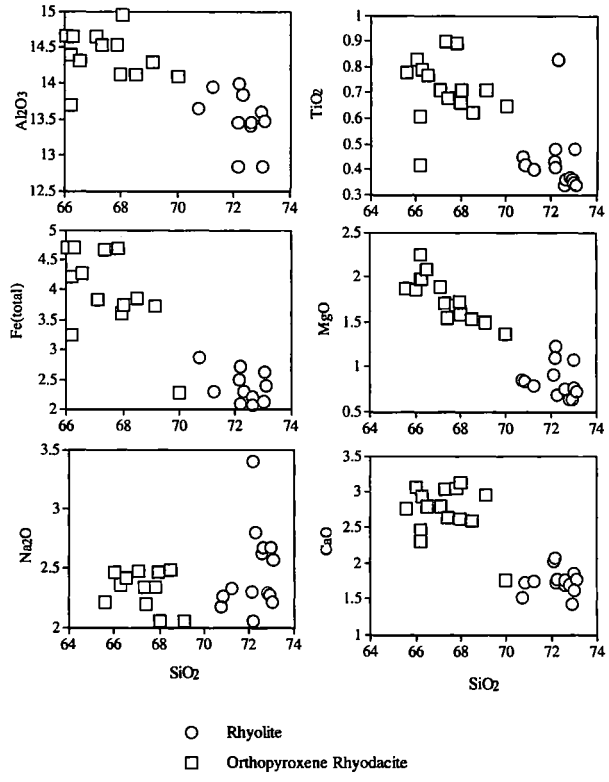

Figure 3: Major element Harker variation diagram for the Sempah volcanic complex

PETROLOGY

Petrographic description of the Rhyolite

Thin section examination shows the rhyolite to be a hypidiomorphic holocrystalline rock consisting of phenocrysts (40–60%) of quartz, plagioclase (andesine), biotite and alkali-feldspar set in an aphanitic glassy groundmass. The groundmass is essentially quarzofeldsphatic with minor occurrences of biotite flakes and Fe–Ti oxides with grains measuring less than 0.2 mm. Texturally the groundmass is tuffaceous consisting of distinctive glass, quartz, feldspar and minor biotite all measuring less than 0.1 mm. There are minor variations in the size of the groundmass in thin section, for example groundmass surrounding most phenocrysts are finer–grained compared to that not associated with reaction rims. There are also individual patches where the groundmass appears to be slightly coarser-grained.

Quartz occurs as phenocrysts and as an essential constituent of the groundmass. Two kinds of quartz phenocrysts are identified: large (2–4 mm) grains and smaller (0.3–0.5 mm) rounded microphenocrysts. Most quartz grains are subhedral and exist as discrete crystals. laths and as angular fragments which vary in size (Phenocrysts range from 1–4 mm whereas microphenocrysts occur in the 0.5–0.7 mm). It also displays albite, Carlsbad–albite and pericline twinning. Both oscillatory and normal zoning were also observed. Determination of anorthite percentage using extinction angles of albite twins in zone 010 show a compositional range from An_{30} – An_{42} (andesine). Sericite is extensively present as an alteration product of plagioclase.

Biotite occurs as euhedral to subhedral phenocrysts up to 5 mm in diameter. It is relatively rare as a groundmass constituent where it occurs as small shreds, which have probably been dislodged from phenocrysts. Although euhedral biotite may be fairly common, the bulk of the biotite is present as ragged elongate shreds. Some biotite phenocrysts, cleaving into sheets separated by groundmass in the rhyodacite, indicate the initial stages in this type of mechanical breakdown. Most biotite flakes are warped to some degree and kink bands are common. The kinking and plastic features observed could have been caused by high-pressure deformation. The pleochroism scheme is typically pale brown to dark reddish brown. Inclusions of biotite in quartz suggest that biotite was an

early crystallizing phase. Chlorite is present as an alteration product of biotite.

Alkali-feldspar (microperthite orthoclase) phenocrysts are often ornamented by internal zones and blebs of groundmass materials, indicative that the grains continued to grow in optical continuity beyond its original outline (Liew, 1977). Microperthite vary in size from 1-4 mm typically displaying embayment structures with various inclusions of accessory minerals and occasional biotite and apatite. Mymerkites are extensively developed where microperthites are in contact with plagioclase, indicating intergrowth at the eutectic composition.

Accessory minerals include apatite and zircon. Apatite is frequently observed as individual blades with near perfect crystal outlines. They occur in almost all phenocryst phases as small (0.1 mm) euhedral-subhedral isolated crystals. Euhedral zircon exists as both discrete individual crystals and as inclusions in biotite.

Petrographic description of the orthopyroxene rhyodacite

Thin-section examination shows the orthopyroxene dacite to be a porphyritic hypidiomorphic holocrystalline rock consisting of phenocrysts (60-70%) of quartz, plagioclase (andesine-labradorite), biotite, alkali-feldspar and hypersthene set in a groundmass consisting of quartz and alkali-feldspar. The groundmass is slightly coarser-grained compared to the rhyodacite. Most of the phenocryst phases display a reaction relationship, except for hypersthene and biotite. Similar to the rhyolite, quartz occurs as phenocrysts and as an essential constituent of the groundmass in the orthopyroxene dacite. Large quartz phenocrysts are subhedral-anhedral with sizes ranging from 2-6 mm, whereas microphenocrysts range from 0.3-0.5 mm and are rounded. Embayments are also present, but not so apparent compared to that of the rhyolite. Apart from the presence of discrete individual crystals, monomineralic clusters of quartz (~0.5 mm each) are abundant, forming elongate patches with triple junction boundaries. Minor calcite veins were also observed intruding quartz crystals.

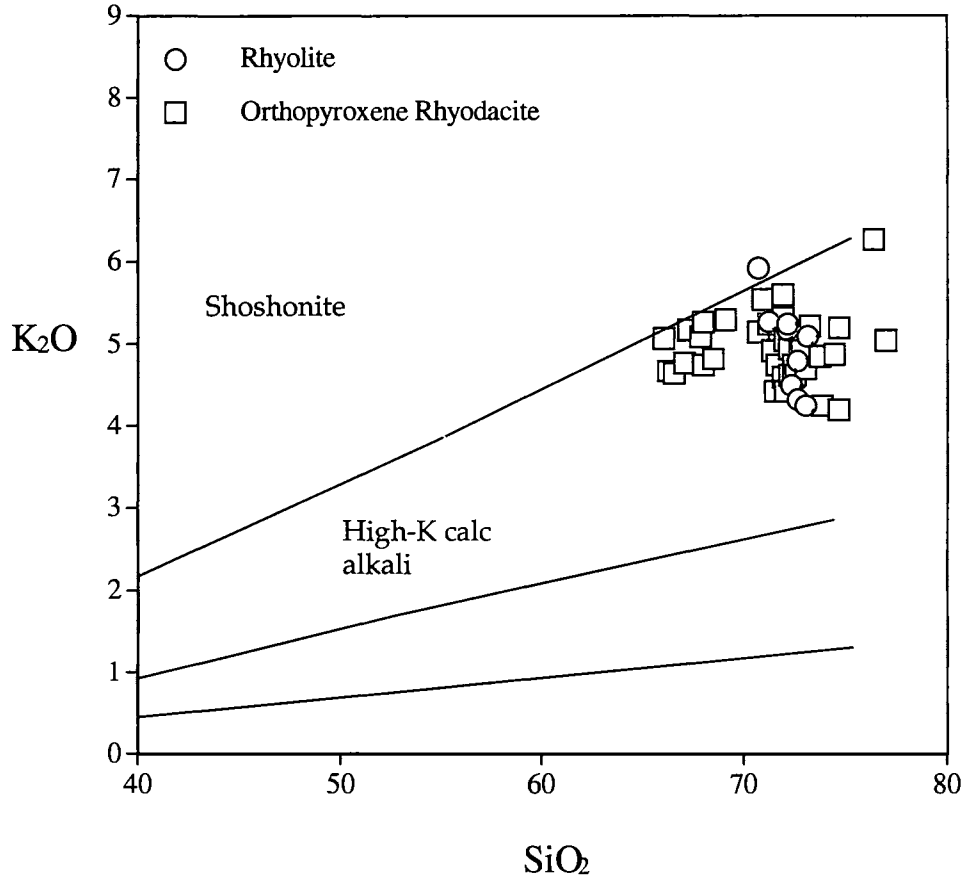

Figure 4: K_2O vs. SiO_2 plot for the Sempah volcanic. There is an increase of K_2O with increasing SiO2 for Rhyolite as opposed to decreasing K_2O values for Orthopyroxene Rhyodacite.

Plagioclase in the orthopyroxene dacite occurs as individual euhedral-subhedral laths, glomeroporphyritic aggregates and very commonly as angular fragments. Phenocrysts range from 1– 4 mm whereas microphenocrysts occur in the 0.4 - 0.7 mm range. Albite, Carlsbad-albite and pericline twinning are all present. Oscillatory and normal zoning were also observed. Determination of anorthite percentage using extinction angles of albite twins in zone 010 show a compositional range from An_{40} (andesine) – An_{54} (labradorite). This is in agreement with Liew (1983) who determined that anorthite contents in cores and rims of zoned plagioclase in the orthopyroxene dacite range from An_{38}–An_{50} based on microprobe analysis. It is inferred that plagioclase was an early liquidus phase having a reaction relationship with evolving melts. This is based on the fact that plagioclase obvious compared to the rhyolite. The pleochroism scheme is typically foxy–red to reddish–brown.

The presence of stumpy subhedral hypersthene in the orthopyroxene dacite is characterized by high relief, low birefringence in sections of normal thickness and parallel extinction. Liew (1977) presented the hypersthene composition range as approximtely $En_{60}Fs_{40}$. Schillerized grains with alligned iron oxides, reaction rims consisting of biotite and Fe-Ti oxides were also observed. Glomeroporphyritic clots of hypersthene in the orthopyroxene rhyodacite suggest accumulation of this phase during crystallization.

Subhedral alkali-feldspar (microperthite orthoclase) range in size from 1–5 mm, displaying embayment structures. Similar to the rhyolite, mymerkites are occasionally developed where microperthites are in

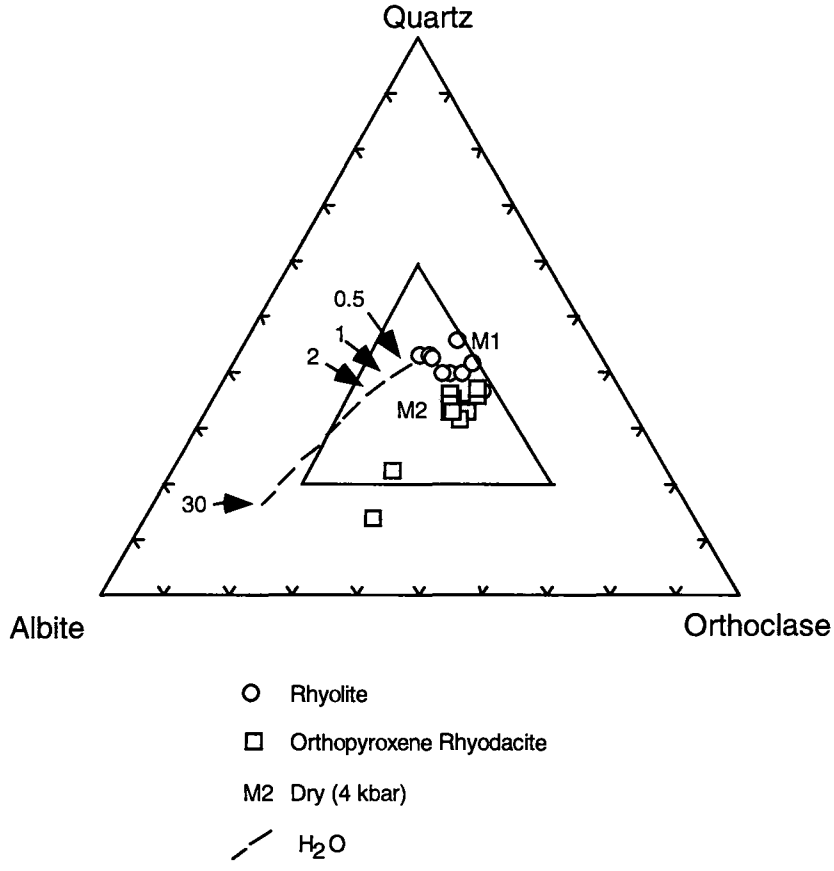

Figure 5: Albite-Quartz-Orthoclase ternary diagram for the Sempah volcanic complex. Inside triangle is the granitoid composition proposed by Tuttle and Bowen (1958)

exist both as discrete phenocrysts, and also as glomeroporphyritic aggregates. Some plagioclases are embayed but generally any corrosion by the groundmass is limited to the production of shallow embayments and serrated and indefinite feldspar margins.

Biotite occurs as euhedral–subhedral phenocrysts between 1–5 mm in diameter and as microphenocrysts measuring 0.5–1 mm. Similar to the rhyolite, it is relatively rare as a groundmass constituent. Kink bands are common, but the degree of deformation observed is less contact with plagioclase. Magnetite is common and apatite occurs as tiny rods scattered throughout all minerals. Zircon is conspicuous as large tabular crystals and as inclusions in biotite. The groundmass consists essentially of quartz and alkali feldspar and is coarser–grained compared to the rhyolite.

GEOCHEMISTRY

Nine (4 : rhyolite and 5 : orthopyroxene rhyodacite) samples were analysed for major and trace elements. In addition to this, a data set of 17 geochemical analyses of

the orthopyroxene rhyodacite and rhyolite has been collected from published and unpublished data (e.g. Liew, 1983; Cobbing et al., 1992). Representative geochemical analysis is given in Table 1. The In general the orthopyroxene rhyodacite is more basic compared to the rhyolite with SiO_2 ranging from 65 – 70.04% and 70.73-74.5% respectively. They are separated by a gap of about 1% SiO_2. The rhyolite also contains significantly lower CaO (1.43-2.07%), MgO (0.64-1.23%), Zr (131-215 ppm), Ba (230-565 ppm) and Sr (68-147 ppm) but higher Rb (313-496 ppm) compared to the orthopyroxene rhyodacite (CaO: 2.63-3.05% ; MgO: 1.55-2.25% ; Zr: 231-294 ppm ; Ba: 770-1021 ppm ; Sr: 128-180 ppm and Rb: 245-368 ppm). The orthopyroxene rhyodacite also contains higher total Fe_2O_3 (2.28-4.7%) compared to the rhyolite, which contain total Fe_2O_3 values ranging from 2.07-2.87%.

With increasing SiO_2, a decrease of TiO_2, Fe_2O_3(total), MgO and CaO is seen for both rhyolite and orthopyroxene rhyodacite (Fig. 3). For the major elements K_2O and P_2O_5, two completely different trends are observed (Fig. 3). On the K_2O vs. SiO_2 plot (Fig. 4), most samples plot in the high-K calc-alkaline and shoshonite field. On this plot, rhyolite decreases whereas orthopyroxene rhyodacite increases with increasing SiO_2. P_2O_5 in the orthopyroxene rhyodacite samples decrease with increasing SiO_2, in contrast to the samples of the rhyolite (Fig. 3).

On a Albite-Quartz-Orthoclase ternary diagram samples of both units are clustered in two separate groups (Fig. 5). It is inferred that both the rhyolite and orthopyroxene rhyodacite had a minimum pressure of 0.5-1kb, which is an indication that both rocks are high-level emplacements (epizonal). The rhyolite plots lie closer to the 0.5 kb point compared to the plots of the orthopyroxene rhyodacite. Rhyolite samples (average Ab/An = 2.33) lie close to the M1 plot suggesting a minimum temperature of 695° C(Winkler, 1967), whereas the average Ab/An ratio for the orthopyroxene rhyodacite is approximately 1.5, suggesting a minimum temperature of 705° C. Based on the water undersaturated system, plots of both rhyolite and orthopyroxene rhyodacite lie very close to the 4kb (dry) point. This suggests that dry water-undersaturated conditions probably prevailed during the crystallization of both rocks. For such dry conditions, dry source rocks are also required.

The ACNK values for the orthopyroxene rhyodacite range from 0.95-1.03, whereas values for the rhyolite range from 1.00-1.36. On the ACNK diagram (Fig. 6), most orthopyroxene rhyodacite samples straddle at the peraluminous-metaluminous boundary. For the rhyolite, there is an increase of ACNK values with increasing SiO_2. All rhyolite samples plot in the peraluminous field and six

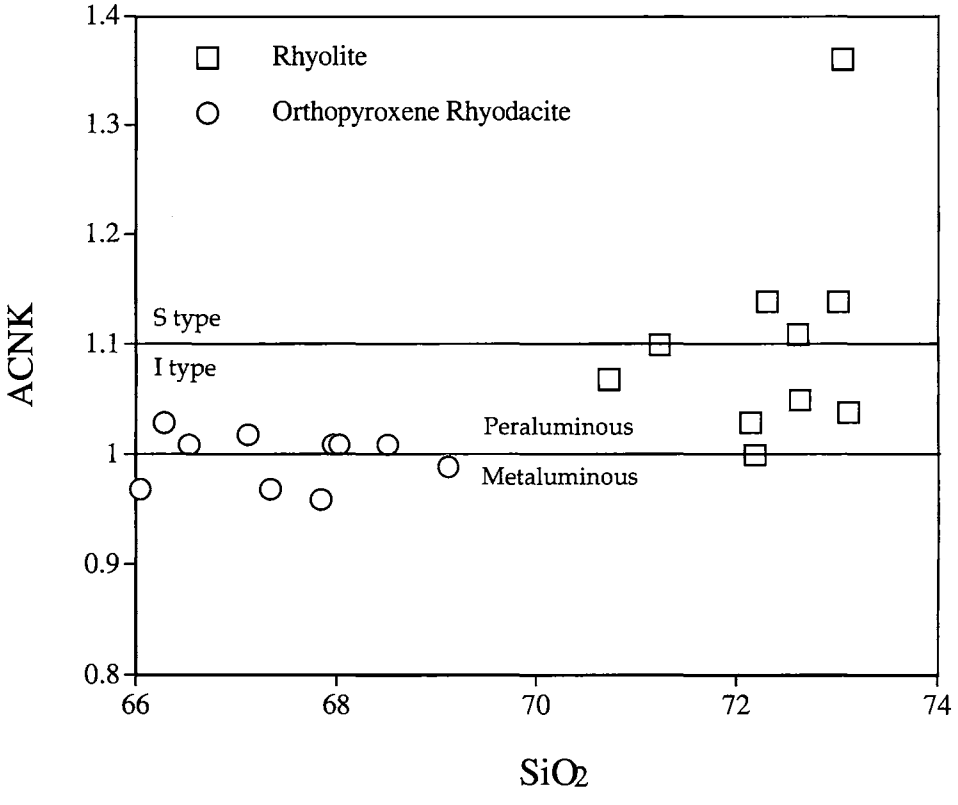

Figure 6: Molar $Al_2O_3/CaO + Na_2O + K_2O$ vs SiO_2 (ACNK) diagram for the Sempah volcanic. A significant observation is the two completely different trends present for both the Orthopyroxene Rhyodacite and Rhyolite. The values for the Orthopyroxene Rhyodacite seem to straddle close to the peraluminous – metaluminous boundary, whereas there is a notable increase of ACNK value with increasing SiO_2

samples plot in the I-type field of Chappell and White (1992). Although there are some samples that appear to be in the I-type domain for the orthopyroxene rhyodacite, most of the samples seem to overlap very close to ACNK=1. On the K_2O vs. Na_2O diagram (Fig. 7) proposed by Chappell and White (1974), the majority of both rock types fall into the S-type field. It can be inferred that the rhyolite and orthopyroxene rhyodacite display S-type affinities. The separate trends for both units also suggest that they are not co-magmatic.

Selected trace element plots is given in Figure 8. Ba, Sr and Zr for both rhyolite and orthopyroxene rhyodacite decrease with increasing SiO_2. The decrease of Ba concomitant with Sr as illustrated in the same figure

specific rhyolite and orthopyroxene rhyodacite. In general, the variation in granitic/rhyolitic rocks can be produced by one of several processes. These include fractional crystallisation, effect of a vapour phase, restite unmixing, magma mixing, crustal assimilation and thermo gravitational diffusion. In the Sempah rocks crystal fractionation appears to be the dominant process that produced the variation within the individual unit. This section attempts to model the geochemistry of the individual units of the Sempah complex as seen at the present erosion level. We have shown that in many of the geochemical plots both rhyolite and orthopyroxene rhyodacite display a different trend which suggest that the magmas may not be related by a simple magma evolution

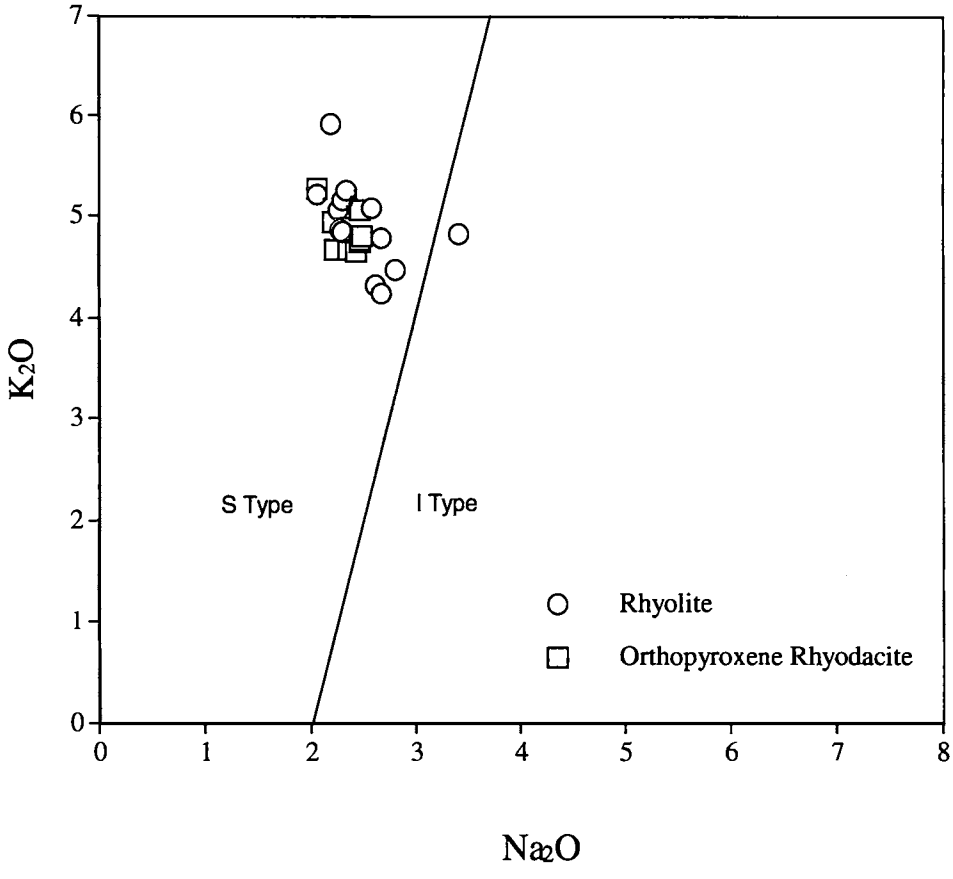

Figure 7: K_2O vs. Na_2O diagram for the Sempah volcanic. Subdivision of S and I type affinities proposed by Chappell and White (1974). Note that majority of the Orthopyroxene Rhyodacite and Rhyolite samples lie in the S type field.

suggests that K-feldspar, biotite and plagioclase are being removed in differentiation sequence. The spider diagram of the trace elements (+K, P and Ti) for the biotite and muscovite granites is shown in Figure 9. Both rocks are depleted in Ba, P and Ti. The depletion of P and Ti is probably related to the apatite and titanomagnetite fractionation. The depletion of Ba is probably related to biotite and alkali feldspar fractionation.

MODELING

The geochemistry of the Sempah rocks shows that they consist of individual melts which later make up from orthopyroxene rhyodacite to rhyolite. Previous study on the Complex suggested that assimilation probably the main cause of the different chemical variation between these two units (Liew, 1977). Within the units, fractional crystallisation appears to be the dominant process that produced the variation of the rocks. Thus in this section, the relation between the two units will be tested using assimilation-fractional crystallization, LIL and major elements modeling.

Assimilation-fractional crystallization (AFC)

Since assimilation requires heat and few magmas are superheated when emplaced in the upper crust, a magma must undergo crystallization in order to fuse crustal material (De Paolo, 1981a). During the process of assimilation, the composition of the parental magma may be modified by crystal fractionation. De Paolo (1981a) and Powell (1984) have derived equations which describe the concentration of a trace element in a melt relative to the original magma composition in terms of AFC processes. The equation for constant values of f and D are:

$$C_L/C_O = f + r/(r\text{-}1+D).\ C_A/C_O(1\text{-}f)$$

$$f = F\text{-}(r\text{-}1+D)/(r\text{-}1)$$

An assimilation-fractional crystallization origin for both units were tested for a number of cases. The modelling of both units shall be treated separately. These tests calculated the trace element trends produced by different combinations of fractionating assemblages. AFC trajectories for progressive contamination of the evolving magmas are presented on a Ba-Sr plot (Fig. 10). Two trends are plotted in accordance with the results of major element modeling.

Trend 1 represents calculated 50% fractionation dominated by biotite, feldspar and orthopyroxene for the orthopyroxene dacite. Trend 2 represents evolution of the rhyodacite controlled by calculated 60% feldspar removal. Bulk distribution coefficients for trend *1* are Sr = 2.5, Ba = 1.5, whereas bulk distribution coefficients for trend *2* are Sr = 2, Ba = 2. Ca values for all calculations are Ba = 350 ppm and Sr = 400 ppm, which are considered average crustal values. The closest fits to the data are then derived assuming a relatively low, but geologically realistic ratio of contamination to fractionation rate of 0.2 (DePaolo, 1981b). It can be observed that the variation for both units can be modelled by AFC processes.

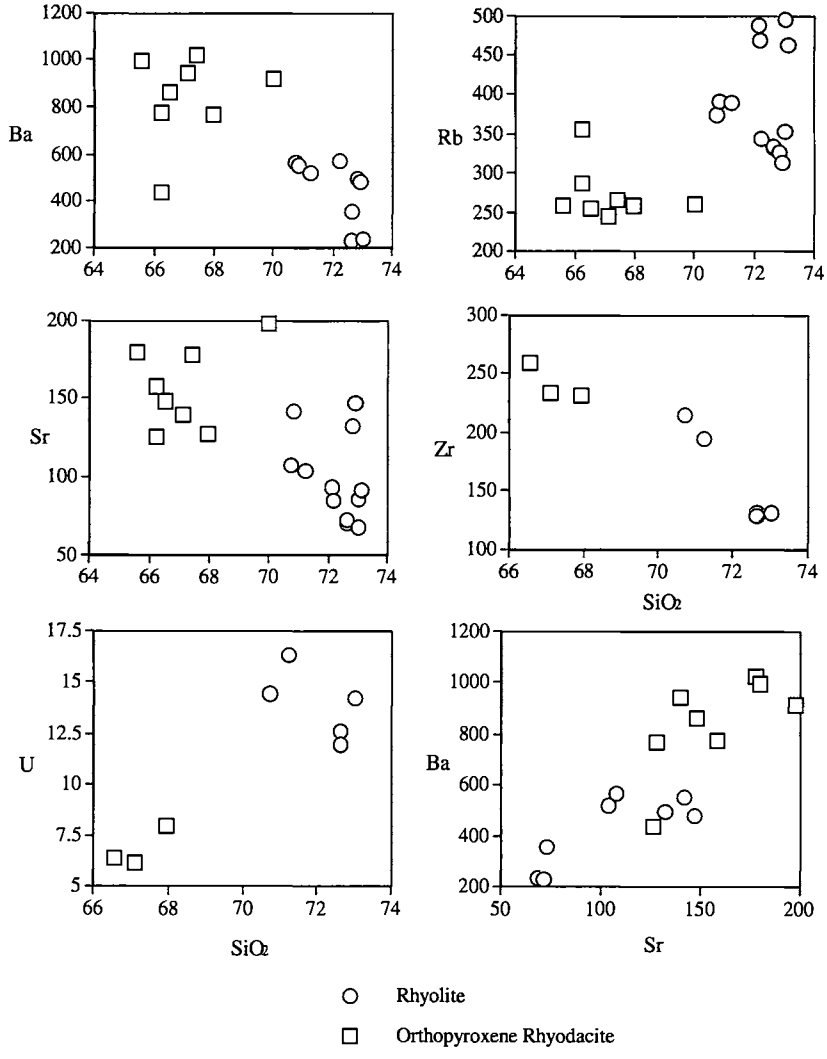

Figure 8: Selected trace elements plot of the Sempah Volcanic Complex.

LIL modelling

The LIL (large ion lithophile) elements Ba, Sr and Rb are of considerable value in determining the type and amount of major phase fractionation in acid rocks because:-

(a) they are held predominantly in the major phases.

(b) partition coefficients for commonly occurring major phases are available.

(c) Each element behaves somewhat differently, for example, Rb is taken up preferentially by biotite, Ba by biotite and alkali feldspar and Sr by plagioclase and K-feldspar.

Mineral partition coefficients of orthopyroxene, biotite, plagioclase and alkali-feldspar for rhyolitic liquids from Rollinson (1993) will be used. On a Ba-Sr diagram for the rhyodacite, a smooth trend is observed within the plagioclase, alkali-feldspar and biotite vector projection for 30% of the mineral phases precipitating (Fig. 11). The vector trend indicates that the fractionation of biotite, plagioclase and alkali-feldspar may be important within the rhyodacite magma. A trend, however, is not observed for the orthopyroxene dacite samples. This could be a result of undersampling (only three orthopyroxene dacite samples with Ba are available).

Isotope interpretation

In this section, the author will attempt to prove that some other process apart from fractionation is the cause of the chemical variation observed in both units. The data obtained for this section is from Bignell (1972) and Liew (1983). A simple plot of measured $^{87}Sr/^{86}Sr$ vs. Sr (Fig. 12a) should reveal the processes influencing the chemical variation. The negative hyperbolic correlation observed indicates that either assimilation or magma mixing can be discerned for both rock types. Crystal fractionation does not change isotopic compositions and should reveal a non-correlative scatter.

Because the parental magma and subsequent hybrid magma have undergone little fractionation, the process of assimilation can be investigated by using $^{87}Sr/^{86}Sr$ vs. 1/Sr systematics (Fig. 12b). On this type of diagram, fractionation generates an igneous suite which plots as a horizontal straight line (Myers *et al.*, 1983). Hybrid lavas formed by crustal assimilation will also plot along a straight line, but in general, it will be non-horizontal. The trends produced by both rocks are not horizontal and thus preclude closed-system fractionation as the main evolutionary process between the two units. The plots also suggest that the rhyolite and orthopyroxene rhyodacite may be related through assimilation.

The author believes that the variation observed in the units can be explained by assimilation and will use this hypothesis as the basis of the following arguments. Measurable isotope variability in volcanic suites suggests

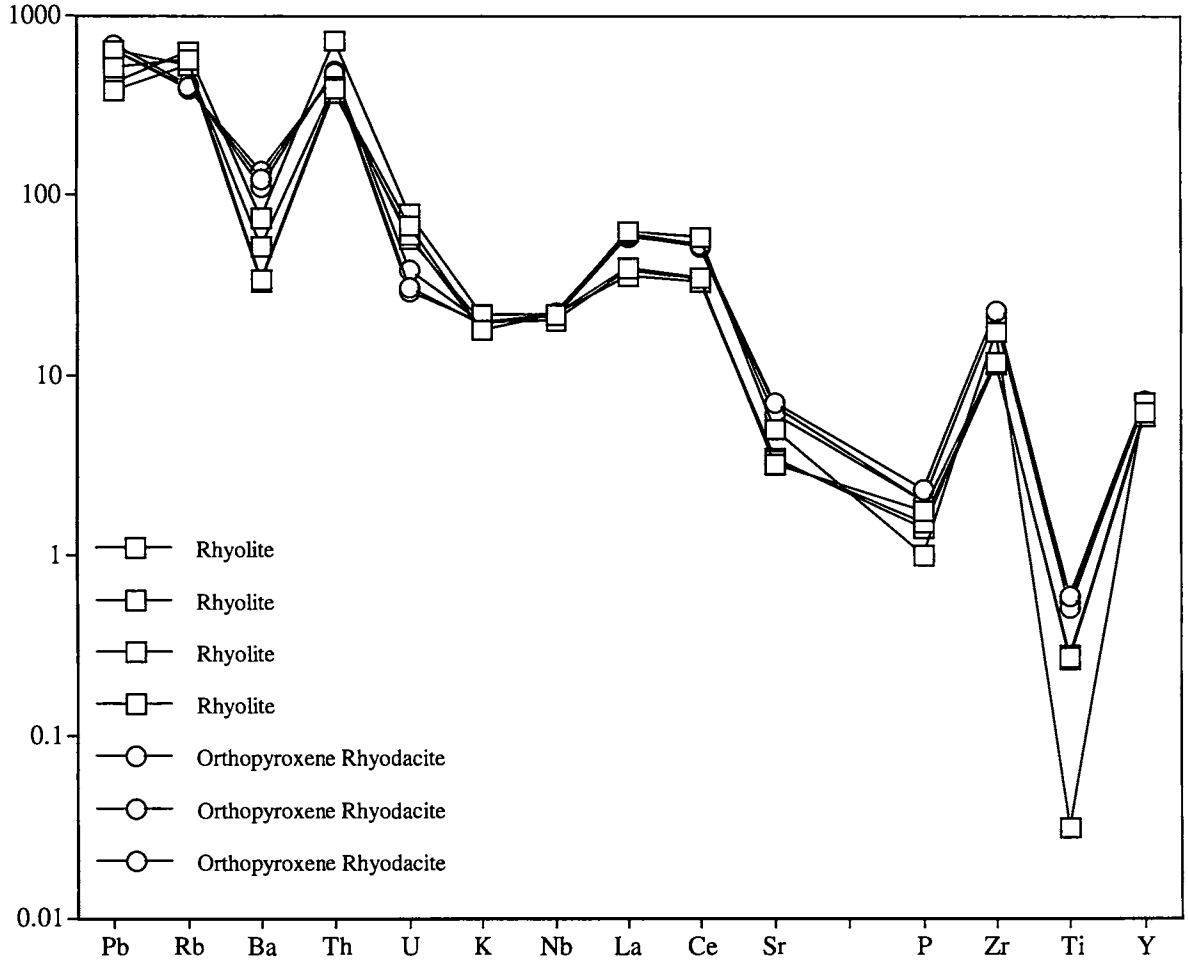

Figure 9: Spider diagram of the Rhyolite and Orthopyroxene Rhyodacite from the Sempah Volcanic Complex

generation by some processes which mixes parental magma with contaminants of different isotopic signature. The isotopic and chemical character of hybrid magmas is a function of the isotopic composition of the two end-members, their relative mixing proportions as well as the degree of concurrent crystal fractionation of the parental magma (De Paolo, 1981a). Typically, isotopic mixing models have been of two general types. The earliest and simplest models assumed fixed parent and contaminant composition (Langmuir et al., 1978). A later model considered the effect of assimilation and crystal fractionation (AFC) of the parental magma on hybrid isotopic systematics (De Paolo, 1981a). The data of the volcanic complex will be discussed in light of these models.

DISCUSSION

The fragmental nature of the phenocrysts in the orthopyroxene rhyodacite and rhyolite cannot be the result of an eruption, as eutaxitic fabrics associated with subaerial activity is not present in the study area. They are more likely to represent an interrupted crystallization sequence for the bulk of phenocrysts. The interruption may have been caused by the quenching of the groundmass at higher crustal levels, or by the invasion of a quartzofeldsphatic liquid into another already crystallizing magma. Most phenocryst phases show evidence of resorption, reaction with groundmass and fracturing. Massive resorption possibly took place as magma was transported to a higher-level chamber. Some phenocrysts (biotite and orthopyroxene) are significantly less resorbed than others. Therefore, it is inferred that magma from different levels in the system got caught up and mixed in with the main batch of rising magma (Shelley, 1993). The

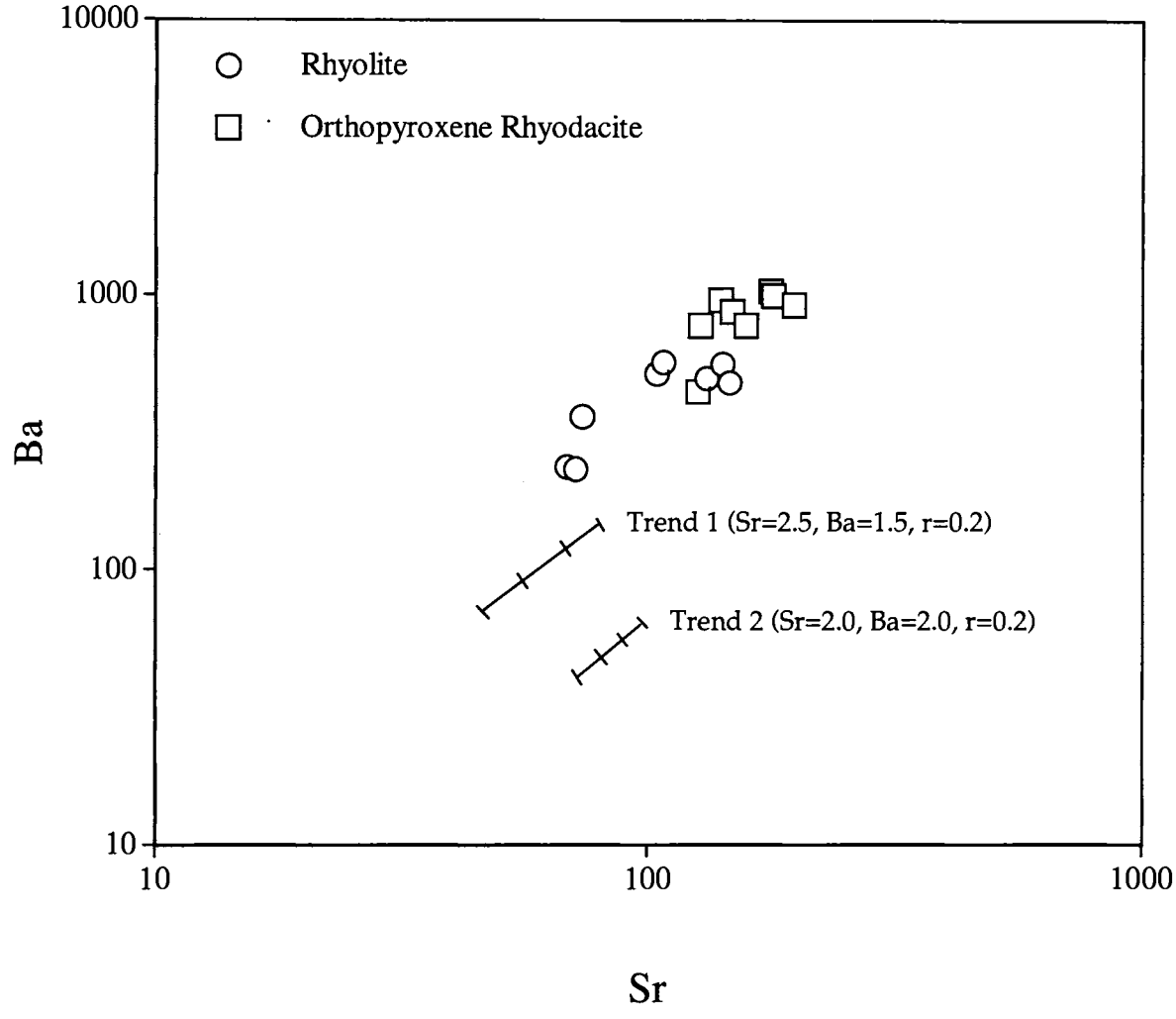

Figure 10: Assimilation-fractional crystallization modeled for Ba-Sr with high grade metamorphic rocks (Ba = 350 ppm, Sr = 400 ppm) as contaminants. Two fractionation stages have been modeled. Trend 1 represent calculated 50% fractionation dominated by biotite, orthopyroxene and feldspars for the Orthopyroxene Rhyodacite (DSr = 2.5 ; DBa = 1.5 ; r = 0.2). Trend 2 represent calculated 60% feldspars removal for the rhyolite (DSr = 2.0 ; DBa = 2.0 ; r = 0.2). The variation samples can be modeled by AFC processes. Tick marks represent propotion of melt remaining in 20% steps

source for both rocks would have most likely been metasedimentary/ sedimentary (S-type), based on the criteria proposed by Chappell and White (1974). Both rocks are inferred to be high-level emplacements based on the Ab-Qu-Or ternary diagram. The plots also suggest that water-undersaturated conditions could have been prevalent during partial melting.

There are distinctive petrographic differences between the orthopyroxene rhyodacite and rhyolite, which are:-

1) the groundmass of the orthopyroxene rhyodacite is generally coarser-grained compared to the rhyolite.

4) the presence of glomeroporphyritic clots is distinctive in the orthopyroxene rhyodacite, but not so apparent in the rhyolite.

The differences seem to indicate that the rocks were not formed by a common magma, which leads the author to infer that the rocks are not co-magmatic. The difference is further support by the K_2O vs. SiO_2 diagram. *In this* diagram the samples from the rhyolite seem to have been evolved from shoshonite to high-K calc alkali fields. Roberts and Clemens (1993) showed that a parent magma with a given K_2O and SiO_2 content will evolve within the particular field in the diagram. For magma to evolve into

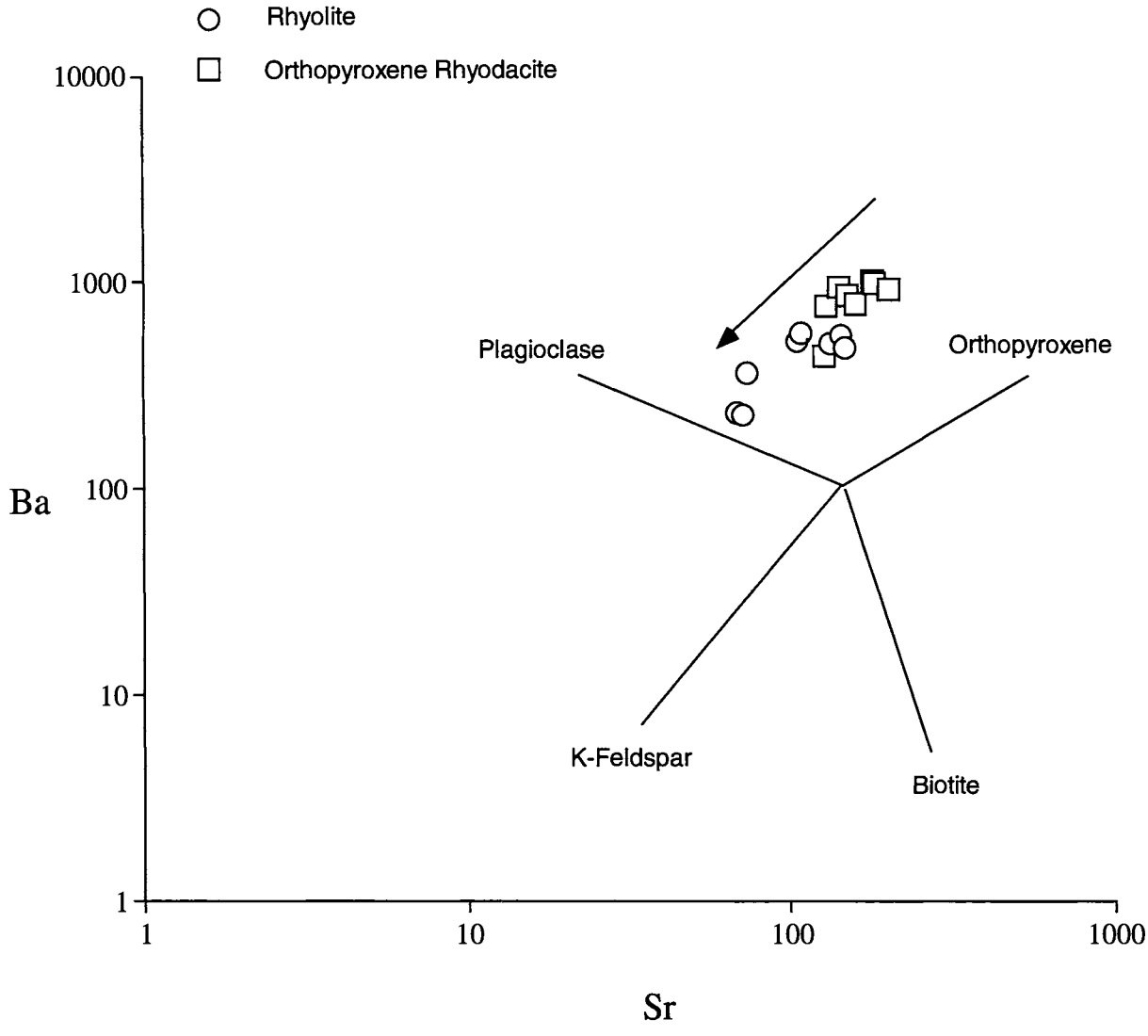

Figure 11: Mineral vector showing fractional crystallization trends in a source containing 200 ppm Sr and 100 ppm Ba. Fractional trends are shown for 30% fractional crystallization of the mineral orthopyroxene, biotite, plagioclase and K-feldspar. The vector displayed for the Rhyolite and Orthopyroxene Rhyodacite samples indicate that the fractionation of plagioclase, K-feldspar and biotite may have played important role in the magmatic evolution.

2) the phenocryst content of the orthopyroxene dacite is higher (>60%) compared to the rhyolite (<60%).

3) the orthopyroxene rhyodacite has distinctive hypersthene and labradorite, which is not present in the rhyolite

an adjacent field some process other than crystal-liquid separation must operate. This clearly is the first indication that the main process governing the chemical variation between both rocks is not simple fractionation. Furtermore plot of Rb vs MgO (Fig. 13) also show a different trend which suggest that both magmas are different. The plagioclase composition in rhyolite is mostly andesine, as

opposed to the combination of andesine-labradorite found in the orthopyroxene rhyodacite. Although the transitional rhyolite porphry appears to texturally resemble the orthopyroxene rhyodacite (except for the presence of hypersthene), the chemical composition of this rock resembles the rhyolite.

The linear variation observed within both units is difficult to reconcile with a purely crystal fractionation model. As crystallization proceeds, phases which are solid solutions should change compositions systematically and this should result in curved trends on variation diagrams (Price, 1983). For example, a fractionation model involving plagioclase cannot readily explain linear variation on an Fe_2O_3(total) vs. CaO diagram (Fig. 14), because the CaO content of the plagioclase being removed decreases as fractionation proceeds and a curved trend should result (Price, 1983). Such a straight line variation is more commonly attributed to hybridization resulting

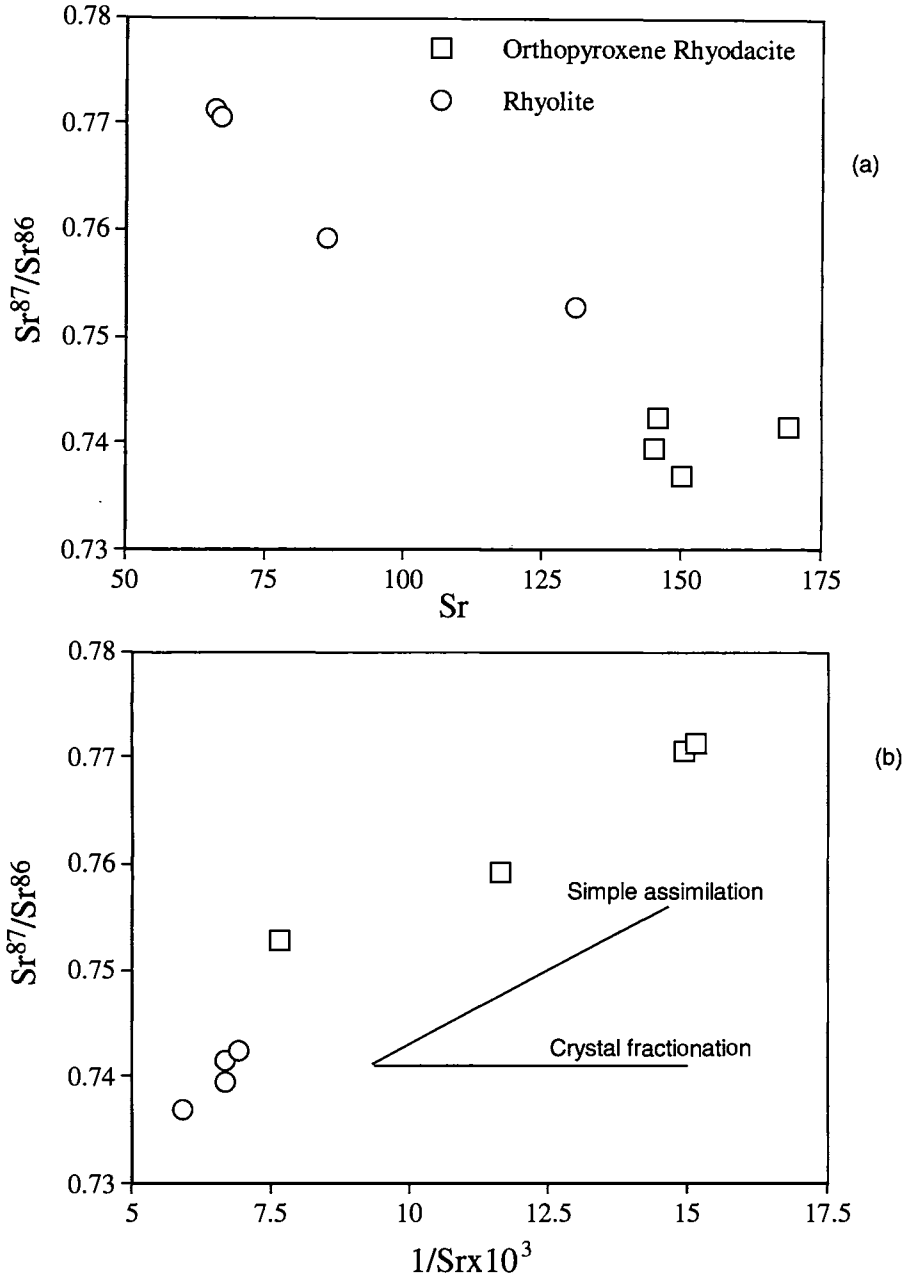

Figure 12: (a) Negative correlation observed for plot measured $^{87}Sr/^{86}Sr$ vs. Sr. A hyperbolic curve is observed for the Rhyolite. A negative hyperbolic correlation indicates that crustal contamination can be discerned not only for the Orthopyroxene Rhyodacite but also for the Rhyolite. Crystal fractionation does not change isotopic composition and should revealed a non-correlative scatter. (b) $^{87}Sr/^{86}Sr$ vs. 1/Sr x 10^3 plot for the Genting Sempah Volcanic Complex. Genarally a horizontal trends is an indication of crystal fractionation, whereas a sub horizontal trendsrepresent a simple assimilation. The trends produce by both Rhyolite and Orthopyroxene Rhyodacite are not horizontal and thus preclude fractionation as the main evolution process between the two units.

either from the mingling of two magmas or the assimilation of wall rock by an uprising magma.

The process influencing the magmatic evolution of both units can be explained by assimilation-fractional crystallization (AFC). High initial strontium isotope values, different mineral extract proportions (major element modeling) and a non-horizontal trend on the $^{87}Sr/^{86}Sr$ vs. 1/Sr preclude crystal fractionation as the main process operating in the complex. This strongly suggests that open system behaviour has been a major control on the evolution of both units. LIL modelling indicates that the removal of alkali-feldspar, plagioclase and biotite to a certain extent, influenced the magmatic evolution within the rhyodacite.

In Figure 15, the multi elements profile of the Sempah Complex rocks is comparable and the Western Belt granites (normalizing values is after Sun and Mc Donough 1989). The Western Belt granite profile was related to fractionation of feldspars, apatite, sphene and Fe-titanium minerals.

CONCLUSIONS

Any model must take into account the following observations:

(i) the absence of hypersthene and labradorite in the rhyolite.

(ii) the relatively high initial $^{87}Sr/^{86}Sr$ isotope values for both rocks.

(iii) high amounts of Ba and Sr in the orthopyroxene rhyodacite compared to the rhyolite.

(iv) a gap of approximately 1% SiO_2 (wt %) observed between the rhyolite and orthopyroxene dacite.

(v) the different magmatic associations displayed by both rocks

During the Late Triassic, crustal extension probably occurred in the vicinity of the current Genting Sempah

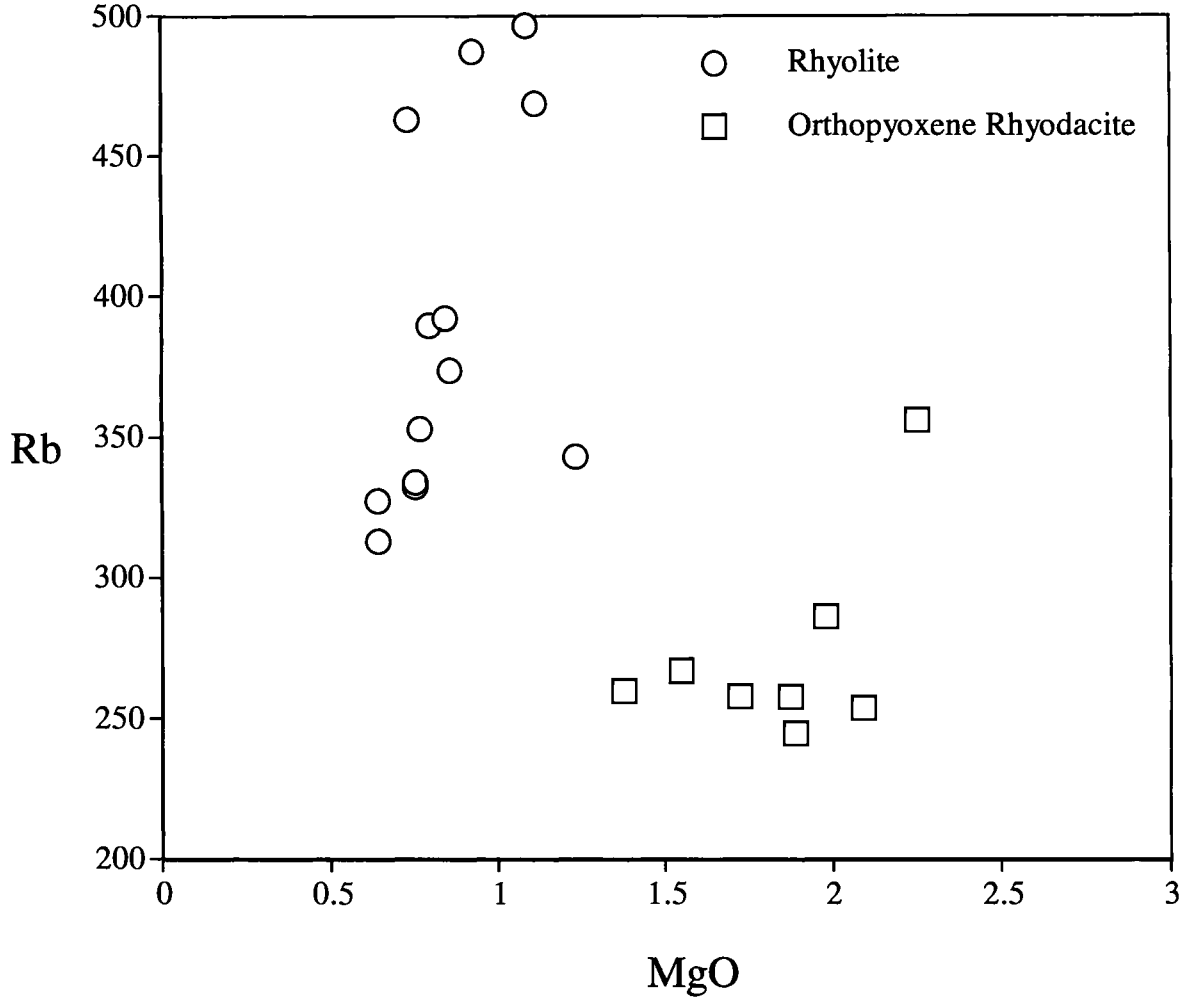

Figure 13: MgO vs Rb diagram of the Rhyolite and Orthopyroxene Rhyodacite from the Sempah volcanic complex

constructed from samples with SiO2 ranging from 67.3% to 76.6% (data taken from Cobbing et al. 1992). The similar profile may suggest the common origin of Sempah Volcanic complex and the Western Belt granites. They are notably depleted in Ba, Sr, P and Ti which is probably area, resulting in a steep geothermal gradient that initiated anatexis of predominantly metamorphic rocks. This resulted in the formation of two separate melts at possibly different crustal levels. The orthopyroxene rhyodacite magma generated at deeper levels based on the occurrence

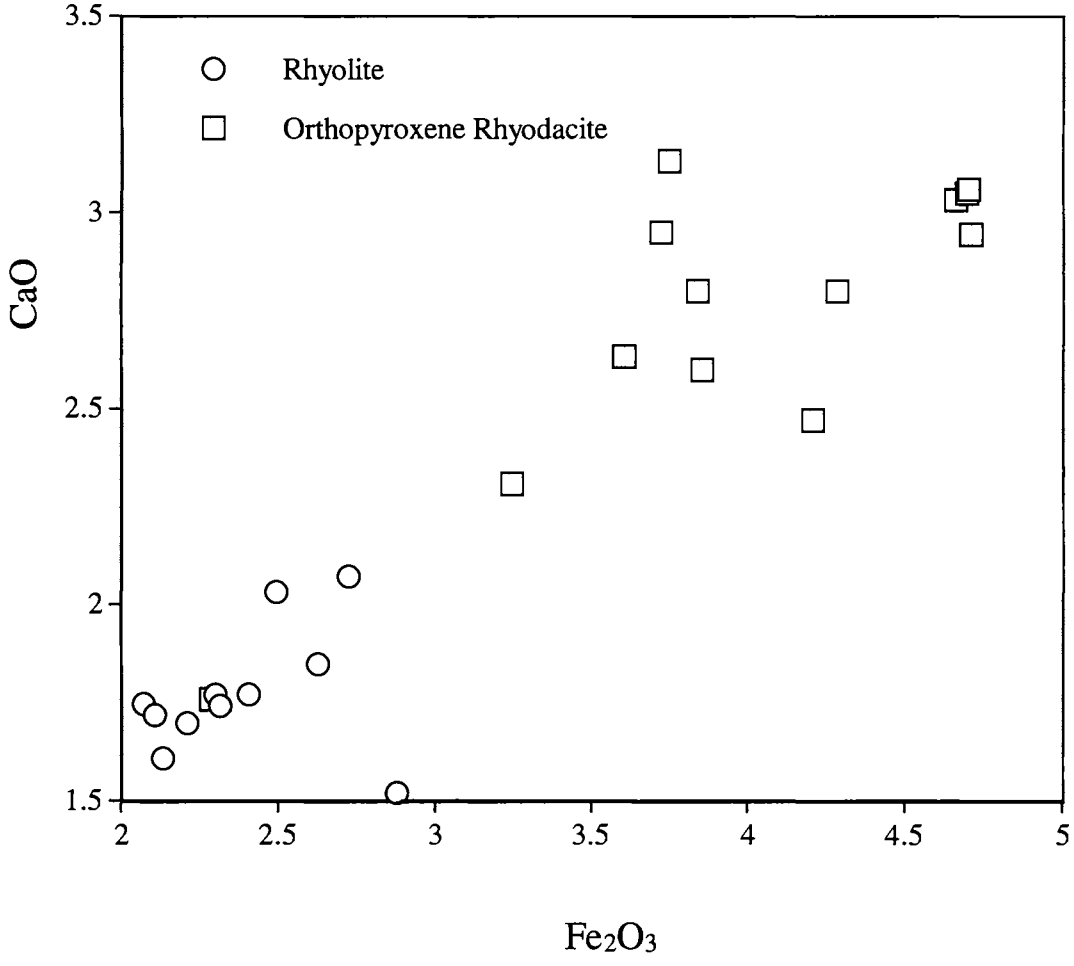

Figure 14: Fe_2O_3 vs CaO diagram of the Rhyolite and Orthopyroxene Rhyodacite from the Sempah volcanic complex

of magmatic hypersthene and labradorite, probably at temperatures of 900 C or more. The rhyolite magma, however, was generated at shallower crustal levels, probably between the temperature regime of 700-800C, based on the absence of hypersthene (Liew, 1983). Since the orthopyroxene rhyodacite displays alumino-cafemic magmatic associations, the strong enrichment of Ba and Sr is probably related to the transfer of hydrous fluids from the mantle.

Both patches of melt were then emplaced at higher crustal levels, while assimilating metamorphic rocks and concurrently experiencing fractionation. AFC modelling indicates that approximately 20% of both magmas were contaminated during emplacement. At the possible depth of 6 km, the orthopyroxene dacite magma which was then assumed to be between 50-60% crystalline underwent rapid undercooling of the groundmass. Water content of the orthopyroxene dacite magma was between 2.5 - 3 wt % with a pressure regime of 3 - 4 kb and a temperature of approximately 800°C when rapid quenching of the groundmass occurred. LIL modelling confirms that plagioclase, alkali-feldspar and biotite did play an important role during the magmatic evolution of the rhyodacite.

Liew (1977) stated that glomeroporphyritic clots of hypersthene and labradorite in the orthopyroxene rhyodacite represent the incomplete breakup of norite, based on jagged and embayed clot margins where they are in contact with the groundmass. Given the fact that hypersthene exists both as glomeroporphyritic clusters and individual phenocrysts, raises the question of whether the individual hypersthene phenocrysts also represent norite inclusions. The author believes that this is unlikely, based on the fact that certain hypersthene phenocrysts are euhedral-subhedral and their margins are not jagged and embayed, implying that some hypersthene crystals did indeed have enough time to precipitate from a melt. They were not caught in the process of being forcefully disaggregated as proposed by Liew (1977). If the norite inclusions represent restite as proposed by Liew (1983), their abundance (< 5% by volume) and distribution precludes any involvement in the generation of the observed chemical variation in the orthopyroxene dacite. The author believes that contamination of the orthopyroxene dacite magma by norite is highly

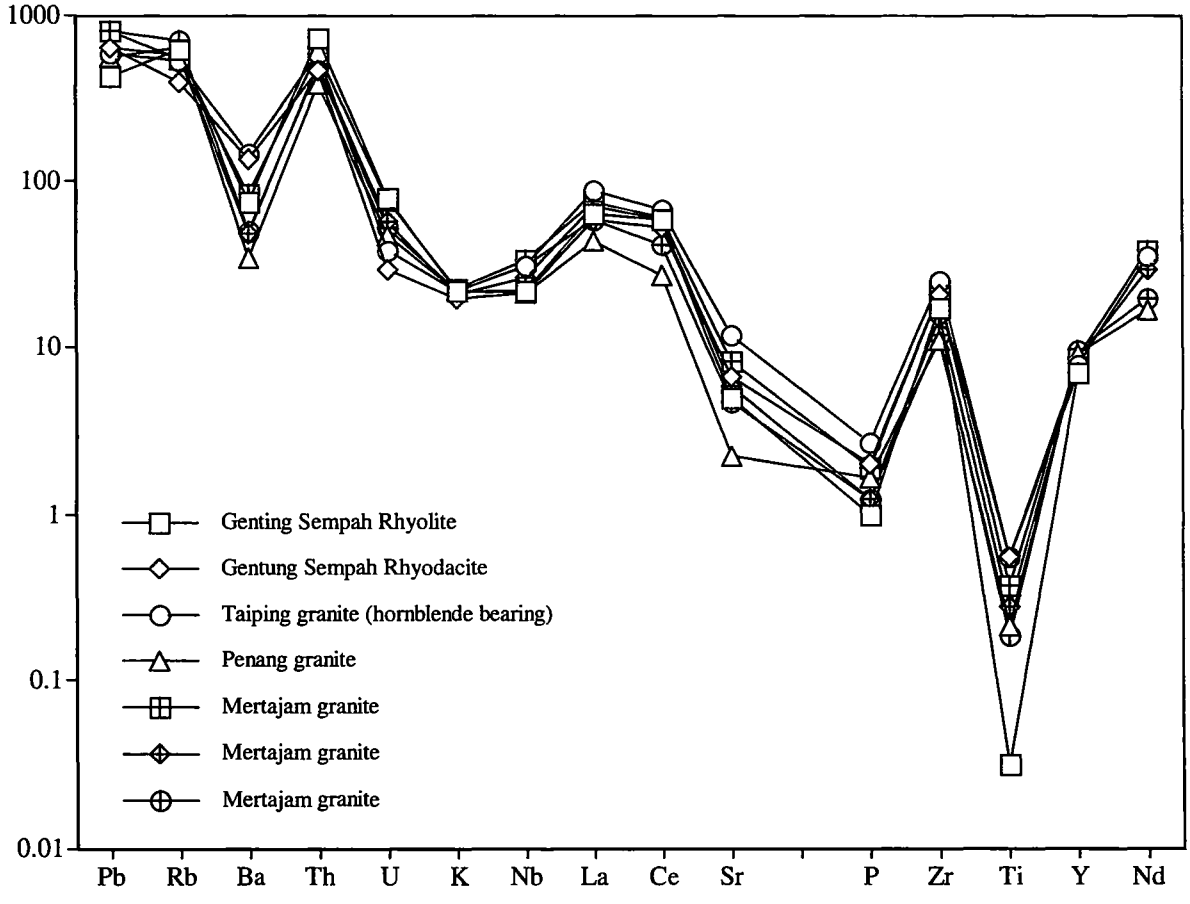

Figure 15: Spider diagram diagram of the Rhyolite and Orthopyroxene Rhyodacite from the Sempah volcanic complex and comparison to other Western Belt Granite.

Sampel No.	MAL 73*	MAL 74*	MAL 75*	MAL 76*	MAL 77*	Liew (6)	Liew (7)	MAL 78*	MAL 79*	MAL 80*	G26
Major Element in w%											
SiO_2	73	72.6	71.22	70.73	72.62	67.32	67.83	66.53	67.95	67.10	70
TiO_2	0.25	0.39	0.2	0.49	0.33	0.39	1.2	1.3	1.67	0.65	0.68
Al2O3	13.6	13.41	13.95	13.65	13.46	14.53	14.54	14.31	14.13	14.65	14.1
Fe(tot)	2.12	2.21	2.31	2,87	2,07	4,66	4,69	4,28	3,6	3,84	2,28
MnO	0.04	0.03	0.02	0,02	0,04	0,08	0,07	0,06	0,05	0,05	0,04
CaO	1.61	1.7	1.74	1,52	1,75	3,03	3,05	2,8	2,63	2,8	1,76
K2O	4.25	4.32	5.26	5,92	4,8	5,17	5,08	4,65	4,75	4,77	4,81
P_2O_5	0.16	0.14	0.09	0,15	0,13	0,22	0,2	0,21	0,18	0,18	0,3
MgO	0.76	0.75	0.79	0,85	0,75	1,71	1,69	2,09	1,72	1,89	1,37
Na_2O	2.67	2.62	2.33	2,18	2,67	2,34	2,34	2,42	2,46	2,47	4,61
SO_3	-	-	-	-	-	0,26	0,29	-	-	-	-
LOI	-	-	-	-	-	0,74	0,74	-	-	-	1,46
S	0.02	-	0.04	-	0,02	-	-	0,1	0,07	0,08	-
H_2O+	1.01	0.97	1.09	0,93	0,82	-	-	0,82	0,75	0,55	-
H_2O-	0.12	0.15	0.15	0,17	0,14	-	-	0,09	0,15	0,17	-
CO_2	0.22	0.15	0.25	0,13	0,28	-	-	0,73	0,29	0,68	-
rest	0.14	0.13	0.19	0,2	0,15	-	-	0,25	0,23	0,25	-
Total	100.07	99.52	99.83	99,77	100,06	100,96	101,41	99,81	99,62	99,83	101
Trace Element in ppm											
Ba	235	230	520	565	360	-	-	860	770	945	-
Rb	353	332	390	374	334	368	348	254	258	245	-
Sr	68	71	104	108	73	153	149	148	128	140	-
Pb	36	27	30	44	45	-	-	45	49	45	-
Th	32.5	31	61	59	33,5	-	-	39,5	40,5	38	-
U	14.2	12.6	16.2	14,4	12	-	-	6,4	8	6,2	-
Zr	132	131	194	215	129	-	-	2,59	231	234	-
Nb	15.5	15.5	15.5	16,5	14,5	-	-	16	15,5	15	-
Y	28	27	32	28	27	-	-	33	31	32	-
la	28	25	45	28	27	-	-	43	42	41	-
Ce	64	60	107	62	62	-	-	97	95	96	-
Sn	21	16	15	13	31	-	-	9	10	8	-
Sc	7	8	8	8	7	-	-	13	11	12	-
V	32	33	35	37	29	-	-	76	61	71	-
Cr	23	23	29	34	21	-	-	57	47	54	-
Mn	345	195	185	125	275	-	-	445	390	415	-
Ni	9	9	13	14	8	-	-	17	15	22	-
Cu	7	5	2	2	6	-	-	12	10	11	-
Zn	40	30	16	18	39	-	-	68	60	76	-
Ga	18	18.2	17	17,2	16,8	-	-	17,6	17,6	17,6	-
Rb/Sr	5.19	4.68	3.75	3,46	4,58	2,41	2,34	1,72	2,01	1,75	-
K/Rb	-	-	-	-	-	140	146	-	-	-	-

Table 1: **Represantative Major and Trace analyses for the Sempah Volcanic Complex**

speculative, since the majority of the Main Range igneous rocks contain SiO_2 between 65-77 wt %. Rocks with SiO_2 ranging < 50 wt % SiO_2 are rare within the Main Range Batholith. Contamination by all means did occur, but the composition and type of contaminant is difficult to constrain.

ACKNOWLEDGEMENT

We would like to thank MTD Prime (Malaysian Thai Development) for allowing us to work along the Karak Highway and Terratech consultants for providing us with a basemap of the highway. This study is partly support by the University of Malaya (Vot F 0523/99B and 0490/2001A).

REFERENCES

ALEXANDER, J.B.,1968. The mineralogy and mineral resources of the neighbourhood of Bentong, Pahang and adjoining portion of Selangor and Negeri Sembilan, incorporating an account of the prospecting and mining activities of the Bentong district. *Memoir Geological Survey Department of West Malaysia 8,* 250 p.

ATHERTON, M.P., MAHAWAT,C. AND BROTHERTON, M.S., 1992. Intergrated chemistry, textures, phase relations and modelling of a composite granodioritic - monzonitic batholith, Tak, Thailand. *Journal Southeast Asian Earth Science, 7 (2/3),* 89 – 112

ATHERTON, M.P., MC COURT, W.J., SANDERSON, L.M., AND TAYLOR, W.P., 1979. The geochemical character of the segmented Peruvian Coastal Batholith associated volcanics. In, Atherton, M.P., Tarney, J. (Eds). *Origin of granite batholiths - geochemical evidence.* Shiva, 45 - 64.

BACON, C.R., 1986. Magmatic inclusions in silicic and intermediate volcanic rocks. *Journal of Geophysical Research, 91,* 6091-6112.

BIGNELL, J.D., 1972. *The Geochronology of the Malayan Granites.* Unpublished PhD thesis, University of Oxford.

BORHAN DOYA, M., 1995, *Petrology and geochemistry of granitoid from Penang, Kedah-Perak and general geology.* B.Sc thesis, University of Malaya, Kuala Lumpur. (In Malaysian)

CHAKRABORTY, K. R., 1995, Genting Sempah volcanic Complex: Genetic implication for the Main Range granite. *Warta Geology, 21,* 216 - 217.

CHAPPELL, B.W. AND WHITE, A.J.R., 1974. Two contrasting granite types. *Pacific Geology 8,* 173 - 174.

CHAPPELL, B.W. AND WHITE, A.J.R., 1992, I- and S-type granites in the Lachlan fold belt. *Transactions of the Royal Society Edinburgh: Earth Sciences 83,* 1-26.

CHOW, W.S, MIOR SALLEHUDDIN MIOR JADID, AND SAZALY YAACOB, 1996. Geological and geomorphological investigation of debris flow at Genting Sempah, Sempah, Selangor. *Forum on Geohazards: Landslides and Subsidence,* 22 nd October 1996.

COBBING E.J., PITFIELD, P. E. J., DARBYSHIRE, D. P. F. AND MALLICK, D. I. J., 1992. The granites of the South-East Asian tin belt. *Overseas Memoir 10, British Geological Survey*

DE PAOLO, D.J., 1981a. Trace elements and isotopic effects of combined wallrock assimilation and fractional crystallization. *Earth and Planetary Science Letters 53,* 189 - 202

DE PAOLO, D.J., 1981b. Sm-Nd, Rb-Sr and U-Th-Pb systematics of granulite facies rocks from Fyfe Hills, Enderby Land, Antartica. *Nature 298,* 614 - 618

HAILE, N.S., 1970. Rhyolitic and granitic rocks around Genting Sempah, Selangor and Pahang, Malaysia, with definition of a proposed new formation, the Sempah Conglomerate. *Abstract Geological Society of Malaysia Discussion Meeting,* Ipoh, December 1970.

HUTCHSION C.S., 1973. Tectonic evolution of Sundaland: A phanerozoic synthesis. *Bulletin Geological Society of Malaysia 6,* 61-86.

HUTCHISON, C.S., 1975. Ophiolite in Southeast Asia. *Geological Society of America Bulletin 86,* 797 – 806

HUTCHISON, C.S., 1977. Granite emplacement and tectonic subdivision of Peninsular Malaysia. *Bulletin Geological Society of Malaysia 9,* 187 - 207.

LANGMUIR, C.H, VOCKE, R.D., AND HANSON, C.N., 1978. A general mixing equation with applications to Icelandic basalts. *Earth and Planetary Science Letters 37,* 380-392.

LEE, S.G., 1976. *Geology of the Genting Sempah area, Selangor – Pahang, with some aspects of geotechnics.* Unpublished BSc (Hons) thesis, University of Malaya.

LIEW, T.C., 1977. *Petrology and structural relationship of rhyolitic rocks and microgranodiorite east of Genting Sempah, Pahang.* Unpublished BSc thesis, University of Malaya.

LIEW, T.C., 1983. *Petrogenesis of the Peninsular Malaysia granitoid batholiths.* Unpublished PhD thesis , Australia National University.

MITCHELL, A.H.G., 1977, Tectonic settings for emplacement of Southeast Asian tin granites. *Geological Society of Malaysia Bulletin 9,* 123 – 140.

MURSYIDAH A. H., AND AZMAN A GHANI, 1999. Kajian terperinci tekstur batuan granit di kawasan Damansara-Sri Hartamas, Kuala Lumpur. *Programme and Abstract of papers, Annual Geological Conference,* Desaru, Johore, 113.

NORMAN, M.D., LEEMAN, W.P., AND MERTZMAN, S.A., 1992. Granites and rhyolites from the northwestern U.S.A.: temporal variation in magmatic processes and relations to tectonic setting. *Transactions of the Royal Society Edinburgh: Earth Sciences 83,* 71 – 81.

PITFIELD, P. E. J., TEOH, L. H., AND COBBING, E. J., 1990. Textural variation and tin mineralization in granites from the Main Range province of the Southeast Asia tin belt. *Geological Journal, 25,* 419 - 430.

POWELL, R., 1984. Inversion of the assimilation-fractional crystallization (AFC) equations; characterization of contaminants from isotope and trace elements in volcanic suites. *Journal Geological Society of London, 141,* 447-452.

PRICE, R.C., 1983. Geochemistry of a peraluminous granitoid suite from north-eastern Victoria, south-eastern Australia. *Geochemical et Cosmochemical Acta 47,* 31-42.

ROBERTS, M. P. AND CLEMENS, J. D., 1993. Origin of high-potassium, calc alkaline I type granitoids. *Geology 21,* 825 -828.

ROLLINSON, H., 1993. *Using geochemical data: evaluation, presentation, interpretation.* Longman, 352 pp

SCRIVENOR, J.B., 1931. *The Geology of Malaya*, London, Macmillan 217 p.

SHELLEY, D., 1993. *Igneous and Metamorphic Rocks under the Microscope*. Chapman and Hall, London, 445p.

SHU, Y.K., 1968. Some NW trending faults in the Kuala Lumpur and other areas. *Newsletter Geological Society of Malaysia 17*, 1-5.

SINGH, N., AND AZMAN A.G., 2000. Sempah volcanic complex, Pahang. In Teh G.H., Pareira, J.J and Ng, T.F. (Eds), *Proc. Ann. Geol. Conf., 2000*, 67 – 72,

SINGH, D. S. AND YONG, S.K., 1982. The localised occurrence of hornblende in granite from the J.K.R quarry, Kuala Dipang, Perak. *Warta Geology 8*, 103.

SUN, S.S., MCDONOUGH, W.F., 1989. Chemical and isotopic systematics of oceanic basalts: implication for mantle composition and processes. In: Saunders A.D., Norry M.J. (Eds) magmatism in ocean basin. *Geological Society of London Special Publication 42*, 315 – 345.

WINKLER, H.G.F., 1967. *Petrogenesis of Metamorphic Rocks*. 2nd edition, Springer-Verlag: New York, 437pp.

Manuscript received 23 February 2005